

# Implications of Photon Mass: Vortextrap Magnetization of Black Holes

Gia Dvali,<sup>1,2</sup> Zaza N. Osmanov,<sup>3</sup> and Michael Zantedeschi<sup>4</sup>

<sup>1</sup>*Arnold Sommerfeld Center, Ludwig Maximilians University, Theresienstraße 37, 80333, Germany*

<sup>2</sup>*Max Planck Institute for Physics, Boltzmannstraße 8, 85748 Garching Munich, Germany*

<sup>3</sup>*School of Physics, Free University of Tbilisi, 0183, Tbilisi, Georgia*

<sup>4</sup>*INFN Sezione di Pisa, Polo Fibonacci, Largo B. Pontecorvo 3, 56127 Pisa, Italy*

We discuss certain astrophysical implications of the photon mass. It offers a new mechanism of black hole magnetization, described as “vortextrap magnetization” (VTM), which can generate a near-saturated magnetic field in astrophysical black holes. The extreme magnetic field is provided by a large number of Nielsen-Olesen type vortex lines piercing a black hole. In massive photon scenario the galactic magnetic field is a densely populated forest of overlapping magnetic flux tubes. These get trapped and collected by a black hole over a cosmological time-scale. The VTM mechanism neatly fits supermassive black holes with sizes matching the phenomenologically-acceptable values of the photon mass, and has implications for magnetic-field based particle acceleration. Even in absence of surrounding plasma, the near-saturated magnetic field is expected to result into an intense electromagnetic radiation as well as gravitational waves in black hole mergers. We provide a numerical simulation of the VTM phenomenon in a prototype system.

## I. INTRODUCTION

The purpose of the present paper is to point out certain astrophysical implications of a non-zero mass of the photon. The mass of photon,  $m_\gamma$ , is a basic microscopic parameter of nature with an uncertain value. Needless to say, any evidence of non-zero  $m_\gamma$  would be of fundamental importance.

Although naively the photon mass is expected to be directly restricted from the uniformity-lengths of the astrophysical magnetic fields of the galaxy and other sources, this was shown not to be the case [1]. The reason is that a non-zero photon mass fundamentally changes the topological structure of the vacuum leading to the formation of Nielsen-Olesen [2] type magnetic vortex lines. An elementary photonic vortex line (or a string) represents a magnetic flux tube of the width given by the photon’s Compton wavelength,  $l_\gamma \equiv \hbar/m_\gamma c$  (where  $c \equiv$  speed of light), with a much thinner Higgs core in the middle. As shown in [1], the vortexes ensure that a strong magnetic field can be effectively Maxwellian over distances  $\gg l_\gamma$ . The reason is that such a uniform Maxwellian field is composed out of large number of vortexes with overlapping magnetic cores.

---

\* gdvali@mpp.mpg.de

‡ z.osmanov@freeuni.edu.ge

§ michael.zantedeschi@pi.infn.it

This finding has the following two effects. On the one hand, it makes the uniformity of the galactic magnetic field fully compatible with values of the photon mass relevant for much shorter scales of astrophysical interest. In particular, the range of  $l_\gamma$  permitted by the scenario of [1], fits the sizes of supermassive black holes.

On the other hand, the vortex structure opens up a new mechanism for generating a strong magnetic field. The maximal strength is determined by the capacity of a given object to hold together a large number of overlapping vortices. We point out that important representatives of this category are black holes. Due to its gravitational pull, a black hole can trap a large number of overlapping flux tubes, thereby, enhancing its magnetic field. We shall refer to this mechanism as the “vortextrap magnetization” (VTM).

The VTM mechanism can be efficient to the extent that in the vicinity of the event horizon the magnetic field might reach the maximal sustainable value,

$$B \sim \frac{c^4}{MG^{3/2}}, \quad (1)$$

where  $M$  is the black hole mass and  $G$  is the Newton’s constant.

Notice that the above expression represents an absolute upper bound on the magnetic field of a black hole, regardless of its origin, which can be imposed from the following energetic considerations. Indeed, we arrive to this value by equipartitioning the gravitational self-energy of a black hole,  $E_{\text{gr}} \sim Mc^2$ , and the energy of the magnetic field,  $E_{\text{mag}} \sim B^2 R^3$ , where  $R \sim MG/c^2$  is the black hole’s gravitational radius. Equating  $E_{\text{mag}} \sim E_{\text{gr}}$ , gives (1). This bound is universal, independently of the value of the photon mass. However, the existence of a non-zero photon mass influences the situation in two ways.

First, in form of VTM it provides a concrete mechanism for sustaining a state with a strong magnetic field due to the collective magnetic flux of photon vortices flowing through a black hole. The strength of this collective field can reach the bound (1).

Secondly, the VTM mechanism suggests that the accumulation by a black hole of the magnetic field above a certain threshold value is expected due to the trapping of the photon vortices encountered during the cosmological evolution. We estimate that the minimal strength of the magnetic field acquired in this way can be rather significant and competing with the values usually assumed to be generated via conventional mechanisms.

The possession of a strong magnetic field by a black hole can result into a number of important effects. In particular, it is of direct relevance for various mechanisms of particle acceleration. The famous examples are the so-called Fermi acceleration [3] with its several modifications [4–6] as well as the Blandford-Znajek mechanism [7, 8].

Another scenario for which VTM has direct implications is so-called magneto-centrifugal acceleration (MA) [9–11]. This mechanism is based on the assumption that plasma particles are in frozen-in conditions, meaning that they follow the rotating magnetic field lines. The role of MA for active

galactic nuclei (AGN) has been studied in a series of papers [9–11] and it was shown that by means of direct centrifugal acceleration, particles might achieve several TeV energies.

Understanding of particle acceleration mechanisms is of particular interest in the light of very high-energy cosmic rays. It is believed that protons with energies  $> 10^{17}$  eV might be produced by AGN [12]. Such protons, when interacting with each other can potentially produce the PeV energy neutrinos [13] detected by the Ice Cube collaboration [14–16]. Recently, the KM3NeT collaboration reported the detection of a 220 PeV neutrino (KM3-230213A) [17], the most energetic neutrino observed to date. This detection further supports the existence of astrophysical accelerators capable of producing cosmic rays and neutrinos at extreme energies. For a comprehensive multi-messenger study of IceCube neutrinos, we refer the reader to [18]. In summary, the study of the origin of ultra high energy protons opens a window also for exploration of astrophysical neutrinos.

In the current work we also point out that a near-saturated value of the magnetic field can have important implications for black hole mergers, since the substantial fraction of the magnetic energy (comparable to a black hole’s gravitational self-energy) is expected to be released in a high-intensity electromagnetic radiation as well as in secondary gravitational waves.

Finally, we illustrate the dynamics of VTM both analytically and numerically on a simple prototype model. In this model the role of a vortex-trapping black hole is played by a solitonic vacuum bubble, which was introduced as an effective description of a black hole in the earlier papers [19–22] within the framework of a so-called “saturon” program. The point is that a class of solitons (referred to as “saturons” in [19]), while being much simpler to analyse, at the same time shares the relevant key features with black holes. Correspondingly, it represents an useful laboratory for understanding the various aspects of the black hole dynamics. The presented analysis of VTM in this prototype system fully matches the expected dynamics in black holes.

We must remark that, besides providing an useful lab for understanding VTM in black holes, the highly-magnetized vacuum bubbles can be interesting astrophysical objects in their own rights, as they can lead to the phenomena very similar to their black hole relatives.

Before proceeding, we would like to clearly isolate the presented VTM mechanism from the alternative scenario of black hole magnetization via vorticity introduced in [21, 22]. In this work it was conjectured that a highly-spinning black hole develops an internal gravitational vorticity which prevents any further growth of the spin relative to the mass. Among other things, this explains the extremality relation between the maximal spin of a black hole and its mass (or entropy). It was also argued that, when interacting with a surrounding plasma, the gravitational vortex can trap a magnetic flux and effectively become a magnetic vortex. Various implications of this scenario such as particle acceleration or primordial magnetic fields require independent studies [23].

Here we wish to comment that the effect of black hole magnetization via the internal gravitational vorticity introduced in [21] is very different from VTM mechanism considered in the present paper. First, the former effect requires a near-maximal spin of a black hole and postulates its connection with internal gravitational vorticity. Secondly, this mechanism is unrelated to the photon mass. In

contrast, the VTM scenario considered in the present work does not rely on the spin of a black hole and also makes no assumptions about possible existence of the gravitational vorticity. In fact, we make no assumptions about the internal microscopic structure of a black hole. Instead, the sole assumption is a non-zero mass of the photon. However, we must say that despite the fundamental differences between the two scenarios, they can have some related implications, in particular for black hole mergers [24], due to the shared predictions of the magnetic vorticity.

The paper is organized as follows. In section II, we discuss the essential features of magnetostatics in the presence of the photon mass and the role of vorticity. In section III, we describe VTM mechanism and show how it can lead to saturation of the bound (1) by a magnetic field of a supermassive black hole. In section IV, we discuss a minimalistic VTM scenario of generation of the magnetic field of a black hole by trapping of vortexes during the cosmological history. In section V, the role of the saturated magnetic field is discussed in light of the multi-messenger physics of black hole merger. In section VI, we illustrate the VTM effect on a prototype system. Finally, in section VII we summarize our results.

Visuals of the dynamics of the VTM mechanism can be found at the following URL.

## II. PHOTON MASS AND MAGNETIC FIELD

In this section, we shall present some relevant information about the photon mass and fix the framework introduced in [1]. We shall use the units  $c = \hbar = 1$ . In particular, in this units,  $l_\gamma = m_\gamma^{-1}$ .

A frequently referred upper bound on the photon mass,  $m_\gamma \sim 10^{-27}$ eV, relies on the coherence length of the galactic magnetic field [25, 26]. The basic assumption in derivation of this bound is that the galactic magnetic field,  $B_g$ , with uniformity length  $l_g$ , would be accompanied by the Proca energy density  $\sim m_\gamma^2 (B_g l_g)^2$ , which is constrained by observations. Notice that this Proca energy would also be constrained by the experiments based on measurements with the toroidally magnetized pendulum in a magnetically shielded vacuum [27, 28], resulting in a milder upper bound  $m_\gamma \sim 10^{-16}$ eV.

However, as it was shown in [1], the above reasoning is not applicable for a very large portion of the theory parameter space, as the existence of the galactic Proca energy is highly sensitive to the microscopic origin of the photon mass. Correspondingly, the uniformity-length of the magnetic field is not directly translatable into the bound on the photon mass. Namely, the would-be Proca energy is cancelled by the winding of the longitudinal polarization of the photon, resulting in formation of vortexes. As a result, the system can support an uniform magnetic field on scales  $l \gg m_\gamma^{-1}$ .

The fundamental reason is that  $m_\gamma \neq 0$  affects the would-be Maxwell theory in the following way:

- The number of degrees of freedom changes discontinuously from 2 to 3, since the massive photon acquires a longitudinal polarization.

- The topological structure of the vacuum changes allowing for the existence of magnetic vortices.
- Due to vorticity, while the electric field is screened at distances exceeding  $m_\gamma^{-1}$ , the magnetic field is not.

Thus, unlike the electric field, the magnetic one is not screened by the photon mass. Instead, the magnetic field is confined into the flux tubes that represent Nielsen-Olesen type vortex lines. The elementary flux tube has the width  $m_\gamma^{-1}$  and can extend to infinity. The multiple overlapping tubes can create a magnetic field with an arbitrarily large coherence length. In order to understand the story let us closely follow [1].

We start with discussing the physical meaning of the photon mass. The Standard Model of particle physics allows for a unique consistent extension of the Higgs effect in which the photon, which we shall denote by  $A_\mu$ , gets a small mass. This requires an additional Higgs field in form of a complex scalar  $\Phi$  with non-zero electric charge <sup>1</sup>. It is convenient to write the field  $\Phi$  in terms of its modulus,  $\rho(x)$ , and the phase,  $\varphi(x)$ , as  $\Phi(x) = \rho(x)e^{i\varphi(x)}$ .

The unique effective low-energy theory describing the massive photon is given by the standard Higgs Lagrangian,

$$\mathcal{L}_{\text{Higgs}} = |D_\mu \Phi|^2 - \frac{1}{4}\lambda^2 (|\Phi|^2 - v^2)^2 - \frac{1}{2}F_{\mu\nu}F^{\mu\nu} \quad (2)$$

where  $D_\mu \equiv \partial_\mu - igA_\mu$  is the covariant derivative and  $F_{\mu\nu} \equiv \partial_\mu A_\nu - \partial_\nu A_\mu$  is the Maxwellian field strength (non-standard normalization is for later convenience). Here  $g$ ,  $\lambda$  are dimensionless coupling constants, whereas the parameter  $v$  has a dimensionality of mass. Notice that  $g$  is a product of the ordinary electromagnetic gauge coupling and the charge of  $\Phi$  which must be minuscule due to phenomenological reasons [1].

In terms of the phase and the modulus fields, the Lagrangian can be rewritten as,

$$\mathcal{L}_{\text{Higgs}} = (\partial_\mu \rho)^2 + (g\rho)^2 \left( A_\mu - \frac{1}{g}\partial_\mu \varphi \right)^2 - \frac{1}{4}\lambda^2(\rho^2 - v^2)^2 - \frac{1}{2}F_{\mu\nu}F^{\mu\nu}. \quad (3)$$

Obviously, the theory exhibits the following  $U(1)_{\text{EM}}$  gauge redundancy,

$$A_\mu \rightarrow A_\mu + \frac{1}{g}\partial_\mu \alpha, \quad \varphi \rightarrow \varphi + \alpha \quad (4)$$

where  $\alpha(x)$  is an arbitrary function.

As it is well-known, the vacuum of the theory is described by a constant vacuum expectation value (VEV) of the modulus  $\langle \rho \rangle = v$ . Correspondingly, the  $U(1)_{\text{EM}}$ -theory is in the Higgs phase.

---

<sup>1</sup> At the level of the full Standard Model, the electric charge of  $\Phi$  originates from its hypercharge. There is no need to enter in this construction, since the low energy effective theory relevant for astrophysical scales is unique (see below).

The would-be Goldstone mode  $\varphi$  becomes a longitudinal polarization of the vector boson and the two form a massive photon field, with the mass  $m_\gamma = gv$ . The fluctuation of the modulus,  $\rho(x) = v + \frac{1}{\sqrt{2}}h(x)$ , represents a massive Higgs boson, with the mass  $m_h = \lambda v$ .

For the phenomenological reasons of non-observation of the  $h(x)$ -boson, the parameter  $g$  must be very small. The parameter  $\lambda$  is less constrained and can be taken all the way up to its perturbative bound  $\lambda \sim 1$ .

At energy scales below  $m_h$ , the effective theory of the massive photon reduces to the Proca theory,

$$\mathcal{L}_{\text{Proca}} = \frac{1}{2}m_\gamma^2 \tilde{A}_\mu \tilde{A}^\mu - \frac{1}{4}F_{\mu\nu}F^{\mu\nu} \quad (5)$$

where  $\tilde{A}_\mu \equiv \sqrt{2}(A_\mu - \frac{1}{g}\partial_\mu\varphi)$  is the massive Proca field.

As it is clear, the longitudinal polarization of the Proca field is originating from the phase of the Higgs field. Notice that the gauge redundancy (4) of the Higgs Lagrangian is fully inherited by the Proca theory. This clarifies a frequent misconception about the breaking of the gauge symmetry by the photon mass. In reality, the gauge redundancy remains intact but becomes hidden due to the gauge-invariance of  $\tilde{A}_\mu$ . In Proca theory the longitudinal polarization of the photon,  $\varphi$ , plays the role of the Stückelberg field which maintains the gauge redundancy of the “parent” Higgs theory (see, e.g., [29]).

The effective Proca Lagrangian (5) is sufficient for accounting for perturbative physics of a massive photon at distances larger than the Compton wavelength of the Higgs field,  $m_h^{-1}$ . However, as pointed out in [1], it is not capable of accounting for some important non-perturbative physics. In particular, in order to understand how the configurations with the magnetic field are affected by a non-zero photon mass  $m_\gamma$ , we must take into account the Nielsen-Olesen vortex lines. For achieving this, one has to incorporate the dynamics of the Higgs field by upgrading the Proca theory (5) into the Higgs theory (3). This non-perturbative physics removes restrictions from the coherence length of the magnetic field, and correspondingly lifts the naive bound on  $m_\gamma$ .

The Nielsen-Olesen vortex lines represent the magnetic flux tubes analogous to Abrikosov vortices in superconductors. The isolated vortex solution with a winding number  $n$  in cylindrical coordinates  $r, \theta, z$  corresponds to the following ansatz,

$$\rho(r), \quad \varphi = n\theta, \quad \text{and} \quad A_\theta(r), \quad (6)$$

with all other components zero. The asymptotic values of the Higgs field are  $\rho(0) = 0$ , and  $\rho(\infty) = v$ , where the asymptotic value  $v$  is approached for  $r > m_h^{-1}$ .

At the same time, for  $r > m_\gamma^{-1}$ , the gauge field  $A_\theta(r)$  approaches a locally-pure-gauge form,

$$A_\theta(r) = \frac{n}{gr}. \quad (7)$$

This results into a magnetic field  $B_z = d_r A_\theta(r)$ . The magnetic flux flowing in  $z$ -direction can be

found from Stokes' theorem and is given by,

$$\text{Flux} = \frac{n}{g}. \quad (8)$$

Correspondingly, the magnetic flux is quantized in units of  $1/g$ .

Thus, the vortex has two cores: the Higgs core of radius  $m_h^{-1}$  and the magnetic core of radius  $m_\gamma^{-1}$ . Correspondingly, the energy of a vortex can be split into the Higgs and magnetic energies. Up to log-factors, both energies per unit length of the vortex line are of order  $v^2$ . This sets the string tension, defined as the energy per unit length of the vortex line, to the value  $\mu \sim v^2$ .

The average value of the magnetic field is,

$$B \sim \frac{n}{g} m_\gamma^2. \quad (9)$$

This formula for the magnetic field is also valid for  $n$  elementary vortexes with overlapping magnetic cores.

While the Nielsen-Olesen vortex configuration is obtained as an explicit solution of the equations of motion, the above behaviour can be understood by balancing the various entries in the two-dimensional energy density functional,

$$\mu = 2\pi \int_0^\infty dr r \left[ (d_r \rho)^2 + \rho^2 (gA_\theta - n/r)^2 + \frac{1}{4} \lambda^2 (\rho^2 - v^2)^2 + B_z^2 \right]. \quad (10)$$

It is clear that the Higgs energy vanishes outside of the Higgs core where we have  $\rho = v = \text{const}$ . Similarly, the magnetic energy vanishes outside of the magnetic core where  $A_\theta$  is given by (7).

The above makes it clear why a non-zero photon mass is not in conflict with the uniformity of the magnetic field over the scales arbitrarily larger than  $m_\gamma^{-1}$ . The reason is that the would-be energy of the vector potential  $A_\theta$  of a magnetic field in the second term of (10) is minimized by the winding of the Goldstone phase  $\varphi$ . That is, instead of restraining the magnetic field, the phase adjusts to it by winding and thereby creating the vortex configurations. As a result, an uniform magnetic field is sustained by a large number of overlapping vortexes [1]. In particular, a homogeneous distribution of the vortexes with  $n$  overlapping magnetic cores, produce the magnetic field of the strength (9).

Following [1], we can understand the essence of the effect as the dynamical lowering of a would-be Proca energy of a constant magnetic field  $B_z = B$  via the vortex formation. In the absence of vortexes, i.e. in the Higgs vacuum with  $\rho = v, \varphi = \text{const}$ , the corresponding vector potential  $A_\theta = Br$  would result into a divergent Proca energy. Namely, within a circle of radius  $R$ , the Proca energy would scale as

$$E_{\text{Pr}} = 2\pi \int_0^R dr r (gv)^2 \left( A_\theta - \frac{1}{gr} d_\theta \varphi \right)^2 = \frac{\pi}{2} (gvB)^2 R^4. \quad (11)$$

However, this energy is cancelled by the winding of the phase  $\varphi$  with the average relation,  $d_\theta \varphi = gBr^2$ .

This implies the existence of uniform distribution of zeros of the Higgs field. They represent the Higgs cores of the Nielsen-Olesen vortices. Around each zero the phase winds by  $2\pi$ . The winding number around a closed circle of radius  $r$  is given by,

$$N(r) = \frac{1}{2\pi} \int d\theta \varphi. \quad (12)$$

Obviously, since the winding number has to be an integer, the cancellation cannot be exact and the residual Proca energy density is  $\sim gBv^2$ . If this energy exceeds the Higgs energy, with density  $E_{\text{Higgs}} \sim \lambda^2 v^4$ , it is energetically preferable for the system to make the Higgs VEV zero everywhere. That is, the magnetic field is sufficiently strong for pushing the Higgs VEV to the top of the Mexican hat potential. In other words, in such a regime the magnetic field un-Higgses the theory.

This fixes the critical value of the magnetic field,

$$B_c = \frac{1}{g} \lambda^2 v^2. \quad (13)$$

For  $B > B_c$  the vortices become so densely populated that their Higgs cores start to overlap. This forms an uniform restored symmetry phase.

For  $B < B_c$  there are different regimes of interest that depend on the size of the system. For  $R > \frac{1}{\sqrt{gB}}$ , the vortices are energetically favourable. However two sub-regimes are possible. For  $R > \frac{\lambda v}{gB}$ , the system classically creates vortices out of the vacuum in order to cancel the Proca energy. In the opposite case  $R < \frac{\lambda v}{gB}$ , the vortices are still energetically favourable but cannot be created classically. Various regions of the parameter space have been explored in numerical simulations [30].

Both regimes are of astrophysical importance. In particular, the photon vortices, that currently make up a particular astrophysical magnetic field, could have been pre-existing in the Universe as a result of an earlier phase transition. Alternatively, they can be created by the magnetic field of an external source such as a star or a galaxy.

For  $v \gg m_\gamma$ , the magnetic cores of the vortices can overlap even if the Higgs cores are far apart. In general, the number  $n_v$  of separated Higgs vortices with overlapping magnetic cores is bounded by

$$n_v \sim m_h^2 / m_\gamma^2. \quad (14)$$

For a higher density of the vortices the Higgs cores start to overlap and the system can enter the un-Higgsed phase as discussed above. For  $n_v$  magnetically-overlapping vortices, the energy cost per area of the magnetic core ( $\sim m_\gamma^{-2}$ ) is  $\mu \sim n_v^2 v^2$ .

Now, the point of [1] is that for  $n_v \gg 1$  the vortices produce a magnetic field which is practically indistinguishable from the Maxwellian case. This lifts the naive uniformity bound on the photon mass. According to this picture, a magnetic field of certain coherence length  $l \gg m_\gamma$ , in reality represents a “forest” of uniformly distributed photonic vortices with overlapping magnetic cores.

In summary [1], the vortex dynamics originating from the photon mass has a dual implication. First, the bounds on the photon mass from astrophysical magnetic fields are lifted, leaving us with milder upper bounds such as the ones coming from the direct measurement of the Coulomb law [31]  $m_\gamma < 10^{-14}\text{eV}$ , or the dispersion of the distant star light  $m_\gamma < 10^{-17}\text{eV}$ . The corresponding Compton wavelengths of photon are within the scales of interest of supermassive black holes.

Secondly, when overlapping in large numbers, the photon vortexes can produce a very intense magnetic field. As we shall discuss next, this overlap, supported by a black hole, can result into a magnetic field strength close to saturation (1).

Before proceeding, let us briefly comment on the gravitational effects of the photon vortexes. An isolated straight and infinite vortex line outside of its core creates a metric of a cosmic string [32]:

$$ds^2 = dt^2 - dz^2 - dr^2 - (1 - 4G\mu)^2 r^2 d\theta^2, \quad (15)$$

where  $\mu \sim v^2$  is the tension. This metric is locally-flat but conical with the angular deficit  $\Delta\theta = 8\pi G\mu$ . If  $n$  parallel vortexes are put on top of each other, the deficit will be controlled according to the collective tension.

For  $m_\gamma^{-1}$  less than the black hole radius, the entire vortex line can go through a black hole. The configuration is expected to be very similar to a black hole pierced by a cosmic string. In thin string approximation, the gravitational metric of such a system was originally given by Aryal, Ford and Vilenkin [33]. Their metric effectively superimposes the string metric on a Schwarzschild background renormalizing the black hole's internal energy due to the string deficit angle.

For us, a particularly relevant case is a black hole with an abelian Nielsen-Olesen vortex studied by Achúcarro, Gregory and Kuijken [34]. This study represents a field theoretic resolution of Aryal-Ford-Vilenkin metric. The black holes pierced by cosmic strings have been further discussed in the literature in various contexts (see e.g., [35–41]).

We must remark that there exists a very general consistency argument [42] according to which a stationary groundstate configuration of a black hole and of an infinite thin string is the one in which the string pierces the black hole. That is, if the two are separated initially, the system will evolve towards the configuration of the black hole pierced by the cosmic string. This argument is based on a version of a black hole no-hair theorem according to which a (semi)classical black hole must couple democratically to all the particle species. In other words, a stationary classical black hole must possess no “species hair” [43–45]. All astrophysical black holes fall under the above constraint.

For  $m_\gamma^{-1} > R$  the black hole can be pierced by the Higgs core, which in the regimes of our interest is much smaller than  $R$ , whereas the magnetic core can spread outside of a black hole. We shall be working in a regime in which the would-be deficit angle is well below  $2\pi$ . Correspondingly, the collective energy of vortexes shall not exceed the mass of a black hole.

Notice that in cases in which the photonic strings captured by a black hole can be substantially long, they can result into a observable double-image lensing effects characteristic to a heavy cosmic

strings. Remarkably, even for a sub-critical magnetic field, e.g.,  $B \sim 10^{-5} B_c$ , the collective lensing effect would be at the current observational bound [46].

### III. BLACK HOLE MAGNETIZATION BY TRAPPING OF PHOTON VORTEXES

In understanding the role of the photon mass for endowing the black holes with strong magnetic fields, we split the discussion in two separate questions. The first step is to understand the VTM mechanism of achieving the highly-magnetized black hole states in case of a massive photon. The second step is the outline of possible cosmological scenarios leading to the formation of such states throughout the Universe’s history. In the present section we shall address the first question.

According to [1], if photon has a Compton wavelength shorter than the uniformity length of a given astrophysical magnetic field, the effectively-Maxwellian field is sustained by a large number of vortexes with overlapping magnetic cores. That is, the Universe is populated by a high density of magnetic vortexes of Nielsen-Olesen type. The density of the vortexes varies in accordance with an ambient magnetic field. Correspondingly, a magnetic capacity of a given object is determined by the ability to accumulate and sustain a large number of overlapping photon vortexes.

In case of a black hole, this capacity is determined by its gravitational power to trap and hold vortexes passing through its interior [33, 34]. Interestingly, there is a curious coincidence that the sizes of supermassive black holes, are around or above the current experimental bound on the photon’s Compton wavelength advocated in [1]. This allows for the phenomenologically-viable scenario of saturation of their magnetic fields by photon’s vortexes.

That is, our basic point is that a non-zero photon mass leads to the existence of black holes pierced by a large number of overlapping “fat” magnetic flux tubes. As we shall estimate, this allows a black hole to possess a magnetic field near saturation (1). We shall not make any assumptions about the microscopic properties of the black hole interior and shall solely rely on known semi-classical features of black hole’s gravity.

We shall consider a situation when overlapping magnetic flux tubes pierce through a black hole of mass  $M$  and radius  $R = 2M/M_{\text{P}}^2$  (where  $M_{\text{P}} \equiv 1/\sqrt{G}$  is the Planck mass). In order to understand the value of the attained magnetic field, we parameterize the gauge coupling of the Higgs as  $g = k m_\gamma/M_{\text{P}}$ , where  $k$  is a parameter, which can be written as,

$$k = \frac{M_{\text{P}}}{v}. \quad (16)$$

Obviously, in all the cases of interest  $k$  is an extremely large number.

Let us explore a black hole of radius  $R$  pierced by  $n_v$  vortexes with overlapping magnetic cores. We wish to estimate the values of  $n_v$  and  $k$  for which the resulting magnetic field saturates the

bound (1). In terms of  $M_{\text{P}}$  and  $R$ , this saturated value can be written as,

$$B_{\text{max}} \sim \frac{M_{\text{P}}}{R}. \quad (17)$$

Equating the magnetic field of  $n_v$  overlapping vortexes to  $B_{\text{max}}$ , we get the condition for saturation

$$B \sim n_v \frac{m_\gamma^2}{g} \sim \frac{n_v}{k} (m_\gamma R) B_{\text{max}}, \quad (18)$$

where we have used (16) and (17).

Thus, the maximal magnetic field is reached for

$$\frac{n_v}{k} (m_\gamma R) \sim 1. \quad (19)$$

Taking into account (14) and (16), this can be translated as the condition on the parameters of the theory,

$$v \sim \frac{1}{\lambda} \left( \frac{g M_{\text{P}}}{R} \right)^{\frac{1}{2}}. \quad (20)$$

For illustrative purposes, we can make further simplified assumptions on the parameters. For example, taking  $\lambda \sim 1$  and  $R \sim m_\gamma^{-1}$ , the equation (20) becomes,

$$v \sim \left( \frac{M_{\text{P}}}{R^2} \right)^{\frac{1}{3}}. \quad (21)$$

Let us explore some numerical examples. We first take  $m_\gamma \sim 1/R \sim 10^{-15}$  eV which is around the experimental bound on the photon mass generated via the Higgs mechanism [1]. This Compton wavelength is of the order of the gravitational radius of a million solar mass black hole ( $R \sim 10^{11}$  cm). From (21) we get  $v \sim$  eV. Correspondingly,  $k \sim n_v \sim 10^{28}$ .

For,  $m_\gamma \sim 1/R \sim 10^{-18}$  eV, (a radius of a billion solar mass black hole) we get  $v \sim 10^{-3}$  eV. Correspondingly the maximal magnetic field is reached for  $n_v \sim k \sim 10^{31}$ .

From the above, it is evident that the magnetic flux tubes in form of Abrikosov-Nielsen-Olesen vortexes originating from the photon Higgs mechanism [1] can support the states of astrophysical black holes close to magnetic saturation (1), or equivalently (17).

As already said, the configuration in which the black hole is pierced by photonic flux tubes can be viewed as an extreme case of a black hole pierced by an abelian Nielsen-Olesen vortex studied by Achúcarro, Gregory and Kuijken [34]. The difference in the present case is that the gauge core of the string in question is unusually “fat” and carries an ordinary magnetic flux. The combined flux can generate the magnetic field close to saturation (17). Of course, for the extreme values of the magnetic field, the back-reaction on the metric becomes significant. However, for order of magnitude estimates the extrapolation of qualitative features of known vortex-black-hole metrics [34] is expected to be valid.

#### IV. A COSMOLOGICAL SCENARIO OF BLACK HOLE MAGNETIZATION VIA VTM

We have seen that the vorticity supported by the photon mass allows for endowing a supermassive black hole with a strong magnetic field via the VTM mechanism. The question how such magnetized black hole states can be actualized during the cosmological evolution requires a separate investigation. Here we shall discuss a basic scenario which must be operative regardless of more involved possibilities. Its essence is that a black hole is expected to trap and accumulate a certain minimal amount of the magnetic flux in form of vortexes collected over its life-time.

Notice that in general all black holes with sizes exceeding the Higgs core of the vortex will be subjected to VTM to certain extents. Within phenomenologically-consistent values of the Higgs mass, this can cover essentially all astrophysical black holes.

Indeed, according to [1], the magnetic field of the galaxy is composed out of high density of overlapping vortexes. These vortexes then are expected to be captured by a black hole upon an encounter. This leads to the enhancement of black hole's magnetic field via VTM.

A configuration of a black hole pierced by a string [33, 34] is expected to be a probable outcome of an encounter between the two. The fact that a thin string trapped by a black hole must be a groundstate of the system is also supported by the general “no-species-hair” arguments [42]. Whether the kinematics of the encounter allows for relaxation to such a groundstate, is a dynamical question. Some dynamical aspects of capture of cosmic strings by a black hole have been discussed previously in the literature [35–39, 47, 48]. The difference in our case is the hierarchy of sizes between the magnetic and the Higgs cores. While a magnetic core can be larger or smaller relative to the size of a black hole, the Higgs core is always taken to be microscopically smaller. We shall assume that upon their encounter the probability of trapping a vortex by a black hole is order one. Basically, we assume that the capture cross section is geometric  $\sim R^2$ .

Thus, the outline of the scenario is the following. First, we adopt the picture of [1], according to which the magnetic field of the galaxy,  $B_g$ , is composed out of a large number of uniformly distributed magnetically-overlapping photonic vortexes. The origin of the galactic magnetic field shall not be our concern. We shall simply take its existence as a fact. The presence of vortexes is not an additional assumption, since, as shown in [1], with the magnetic field in place, its vortex composition is a must.

The number of overlapping photonic vortexes reproducing this field is

$$n_g \sim g \frac{B_g}{m_\gamma^2}. \quad (22)$$

A black hole of radius  $R$  moving through this vortex forest, collects them upon the encounter.

Here we need to differentiate among the black holes of solar and intermediate masses, which can travel through the galaxy, and the supermassive ones that are “stationed” near the center. However, in both cases we assume that the encounter between a black hole and the vortex network shall take

place due to the relative motion. That is, even a stationary black hole is expected to be subjected to a “wind” of the vortex lines due to the cosmological evolution of the network.

Assuming that the probability of capture is order one, after traveling a relative distance  $l \gg R$ , the number of collected vortexes by a black hole is,

$$n_c \sim (l R m_\gamma^2) n_g \sim g(l R) B_g, \quad (23)$$

where the factor  $(l R m_\gamma^2)$  is the transverse area swept by a black hole in units of the cross section of vortex’s magnetic core.

On the other hand, the required number of vortexes piercing the black hole that would produce the saturated magnetic field  $B_{\max}$  (17) is,

$$n_v \sim g \frac{M_{\text{P}}}{R m_\gamma^2}. \quad (24)$$

This gives,

$$\frac{n_c}{n_v} \sim \frac{l B_g}{M_{\text{P}}} (R m_\gamma)^2. \quad (25)$$

This fraction measures the accumulated magnetic field  $B$  relative to the maximal attainable value  $B_{\max}$ . Therefore we can write,

$$B \sim \frac{l B_g}{M_{\text{P}}} (R m_\gamma)^2 B_{\max}. \quad (26)$$

Now, the length of the traveled path by a black hole relative to the vortex network throughout the Hubble time  $t_{\text{H}}$  can be estimated as  $l \sim 10^{-4} t_{\text{H}}$ . Numerically this gives,

$$\frac{n_c}{n_v} \sim 10^{-6} (R m_\gamma)^2. \quad (27)$$

Thus, from this mechanism, over a cosmological time a black hole can accumulate the magnetic field of the following value,

$$B \sim 10^{-6} (R m_\gamma)^2 B_{\max}. \quad (28)$$

We must reiterate that the value given above represents a minimal estimate of the magnetic field expected to accumulate around a black hole over its lifetime due to its exposure to a dense forest of photonic vortices. In our analysis, we assume that the black hole propagates through a region with an uniform magnetic field throughout its cosmological evolution. Namely, we assume that the black hole travels within the magnetic field of the galactic coherence length, over time  $t_{\text{H}}$ .

Obviously, validity of this assumption depends on the object’s precise trajectory as well as the cosmological evolution of the magnetic field. In particular, the black hole may enter regions containing vortices with opposite winding numbers compared to those it has already trapped. This

would lead to the capture of oppositely wound vortices, which could then annihilate with the pre-existing trapped magnetic fields. The detailed characterization of the imprints of this dynamical process is left for the future work.

Additionally, astrophysical black holes are always surrounded by plasma, which can further enhance the magnetic field. More sophisticated and model-dependent mechanisms could certainly be considered, but such an analysis is beyond the scope of this work.

In this respect we wish to comment on an important difference between the Higgs/Proca type fundamental mass of the photon and its effective “mass” acquired from the interaction with the astrophysical plasma. Surely, propagation through an ionized medium generates an effective screening length which in certain aspects has an effect similar to a mass. However, there are dramatic differences between the effective mass generated in this way and the fundamental mass of a photon discussed in [1] and in the present work.

First, unlike the Higgs vacuum, the ionized inter-stellar medium is not a superconductor. Correspondingly, sustaining a stationary magnetic field requires an external source. This applies to the magnetic flux trapped in a vorticity generated in such a medium. Even if the flux-carrying vorticity is generated in ionized plasma, maintaining it requires a constant external support. Without it, the vorticity shall cease to exist and the magnetic flux will spread and dissipate. The story is fundamentally different in case of the photon mass generated via the Higgs mechanism, for which the existence of vorticity is the vacuum effect.

Moreover, the Higgs vacuum is different from an ordinary superconducting medium, as there are no actual particles in the vacuum condensate. Due to this feature, the Higgs vacuum is Poincare-invariant and the photonic vortexes are originating from its non-trivial topological structure. The Higgs core plays an absolutely crucial role both in maintaining the magnetic flux tubes without any external help as well as in their trapping by a black hole.

## V. IMPLICATIONS OF VTM FOR MULTI-MESSENGER PHYSICS OF MERGER

We would like to briefly mention a rather straightforward potentially-observable implication of a VTM-generated near-saturated magnetic field for black hole mergers. During the merger it is expected that a substantial fraction of the magnetic energy will be released in form of the electromagnetic radiation. Crudely, this process can be thought of as inter-commutation of magnetic flux tubes piercing the black hole with subsequent formation of closed flux lines and their decay into electromagnetic waves.

For a saturated value (1), during the latest stage of the merger, the power of emitted radiation can be nearly Planckian,

$$L \sim \frac{M_{\text{P}}c^2}{t_{\text{P}}} \sim 10^{59} \text{ erg/s}, \quad (29)$$

where  $t_P \equiv \sqrt{\hbar G/c^5}$  is the Planck time and we temporarily reintroduced  $\hbar$  and  $c$ . This energy is expected to be released in electromagnetic radiation of wavelength  $\sim R$  of extremely high intensity. For example, for  $M \sim 10^9 M_\odot$  the occupation number of the emitted photons per wavelength  $R \sim 10^{14}$  cm is about  $N_\gamma \sim 10^{95}$ <sup>2</sup>. This electromagnetic radiation shall also source the secondary gravitational waves.

In the next section we illustrate the effect of the high-intensity electromagnetic radiation during the merger in a numerical simulation performed on a simple prototype model which makes the essence of the phenomenon very transparent. This analysis confirms the qualitative expectations given above. The analysis of observational prospects is beyond the scope of the present paper, however, the saturated magnetic field is expected to make an order-one difference in the dynamics of the merger.

## VI. SIMULATIONS OF VTM IN A SIMPLE PROTOTYPE MODEL

### Analytcs

In this section we explicitly illustrate the VTM mechanism on a simple prototype model that, while capturing the key features of the mechanism, is easier to understand and solve both analytically and numerically. This general approach of simulating the dynamics of black hole physics in soliton systems was used in several publications [19–22, 50–52] and relies on the finding that the fundamental features of black holes are shared by a large class of solitonic objects, the so-called “saturons” [19]. The defining feature of this class of objects is the maximal microstate degeneracy. This correspondence allows to analyse many dynamical aspects of black hole physics by using such solitons as laboratories.

In the present context we use this method for studying the VTM effect. The idea is to replace a black hole with a prototype soliton possessing a similar trapping power of the electromagnetic vortex. This role shall be assigned to a vacuum bubble separating the phases with broken and unbroken global symmetries [19] stabilized by the internal charge [20–22].

In order to achieve this, we introduce the additional scalar field  $\Sigma$  and add the following terms to the Lagrangian (2)

$$\mathcal{L}_\Sigma = \text{Tr}(\partial_\mu \Sigma)^2 - V(\Sigma) - \beta^2 (\text{Tr} \Sigma^2) |\Phi|^2, \quad (30)$$

---

<sup>2</sup> Notice that by no means the Planckian power of the emission should be understood as if the emission process represents a probe of quantum gravity in Planck scale regime. The wavelengths of the emitted photons  $\sim R$  are macroscopic and correspondingly their energies  $E_\gamma \sim \hbar c/R$  are much less than the Planck energy  $M_P c^2$ . The high power of radiation is a result of a very high amplitude, or equivalently, of a high occupation number of photons  $N_\gamma$ . Correspondingly, the quantum gravitational effects are totally negligible and the emission process is well within the validity of classical gravitational physics. For a general discussion clarifying the dependence of the strength of quantum gravitational effects on wavelengths of quanta versus field intensity/occupation numbers, the reader is referred to [49].

where  $V(\Sigma)$  is the self-interaction scalar potential of the  $\Sigma$ -field, whereas the last term describes the cross coupling between  $\Sigma$  and  $\Phi$ . Of course, it is assumed that all terms are invariant under the symmetries acting on  $\Sigma$  and  $\Phi$ .

Both the internal quantum numbers of  $\Sigma$  as well as the structure of  $V(\Sigma)$  are chosen in such a way that  $\Sigma$  supports a continuous spectrum of the stable solitons [20–22]. The simplest class of such solutions emerges when  $\Sigma$  carries a charge  $Q$  under some global symmetry and  $V(\Sigma)$  has two degenerate vacua with  $\Sigma = 0$  and  $\Sigma \neq 0$  respectively. Obviously, these vacua correspond to the phases with unbroken and broken  $Q$ -symmetry respectively. In [19–22], the field  $\Sigma$  was chosen to transform as an adjoint representation of a global  $SU(N)$ -symmetry with  $Q$ -charge identified with one of its generators. We shall use this example in numerical simulations below. However, the VTM phenomenon is independent on the representation content as long as the above-discussed general conditions are satisfied.

Following [20–22], without any loss of generality, we can parameterize the  $\Sigma$ -field as a complex scalar  $\Sigma(x) = \sigma(x)e^{i\chi(x)}$  with modulus  $\sigma$  and the phase  $\chi(x)$  and reduce the system to its bare essentials via the following effective Lagrangian,

$$\mathcal{L}_\Sigma = (\partial_\mu \sigma)^2 + \sigma^2 (\partial_\mu \chi)^2 - \alpha \sigma^2 (\sigma - f)^2 - \beta^2 \sigma^2 \rho^2, \quad (31)$$

where  $\alpha$  is the coupling and  $f$  is a scale. Obviously, the potential has two degenerate minima, with the VEVs  $\sigma = 0$  and  $\sigma = f$  respectively. In the vacuum with broken symmetry,  $\chi$  describes a massless Goldstone field, with the coupling (Goldstone decay constant)  $1/f$ , whereas the perturbation of  $\sigma$  has a mass  $m_\sigma^2 = \alpha f^2$ .

This system possesses the vacuum bubbles of broken symmetry which have large internal Goldstone degeneracy [19]<sup>3</sup>. It has been further shown in [20] that the vacuum bubble is stabilized due to its internal rotation by the broken symmetry generator, similarly to a non-topological soliton or a  $Q$ -ball [53, 54]. In spherical coordinates, the field configuration has the form,  $\Sigma = f(r)e^{i\omega t}$ , where  $f(0) \neq 0$  and  $f(\infty) = 0$ . The parameter  $\omega$  is arbitrary and determines the mass,  $Q$ -charge and the size of the bubble.

In order to match the regimes of interest motivated by astrophysical black holes, we shall work in a small back-reaction limit which is given by

$$\beta v \ll m_\sigma \quad \text{and} \quad v \ll f. \quad (32)$$

This choices guarantee that the influence from the Higgs VEV on the bubble solution is negligible and the bubble is heavier than the energy of the elementary vortex line of the same size. This is

---

<sup>3</sup> Remarkably, for the highest global symmetry permitted by unitarity (which for  $SU(N)$  is saturated for  $N\alpha = 1$ ) the bubble saturates the same universal bound on the microstate entropy as the black hole modulo the mapping  $f \rightarrow M_{\text{P}}$  [19–21]. This property is the key to the black hole/saturon correspondence [19–22, 50–52]. While this feature is unessential for the VTM mechanism, it further strengthens the motivation for using the above soliton as a test lab.

fully justified, since, translated to the gravitational counterpart, the condition (32) maps on the features that the Higgs vacuum does not affect the black hole and the vortex line is lighter than the black hole.

Next, for clarity we shall start with the approximation of a thin-wall and then move to a generic case. This implies that the bubble radius  $R$  is much larger than the wall thickness which is given by the inverse mass of  $\sigma$ ,  $R \gg m_\sigma^{-1}$ . The mass  $M$  and the radius  $R$  of a stable thin-wall bubble are related as [20],

$$R \simeq \frac{M}{\pi f^2} \frac{1}{m_\sigma R}. \quad (33)$$

Notice that for a thick wall bubble,  $m_\sigma R \sim 1$ , the above relation coincides with the analogous relation between the black hole mass and the radius, with  $1/f^2$  playing the role of the Newton's constant (or equivalently,  $f$  assuming the role of  $M_{\text{P}}$ ). This feature is no accident and lies in deep universality of saturon solitons and black holes [19–22, 50–52]. We shall not enter further in this correspondence but shall only use the bubble as a laboratory for illustrating the VTM mechanism.

A thin-wall bubble represents a sphere of vacuum  $\sigma = f$  embedded in the vacuum  $\sigma = 0$ . We shall study the interaction between the bubble and the photonic vortex-line produced by  $\Phi$ . In the small back-reaction limit (32), the influence of the bubble on the Higgs field can be found by minimizing the effective potential of  $\rho$  in the background of the bubble,

$$V_{\text{eff}}(\rho) = \beta^2 f(r)^2 \rho^2 + \frac{\lambda^2}{2} (\rho^2 - v^2)^2, \quad (34)$$

where we have substituted  $\sigma$  with the bubble profile function  $f(r)$ .

The vacuum outside the bubble,  $r > R$ , where  $f = 0$ , is identical to the previously-considered Higgs vacuum with the VEV of  $\rho$  given by,  $\rho_{\text{out}} = v$ . Correspondingly, this vacuum supports the Nielsen-Olesen vortex-lines as discussed above. The tension of the vortex line is  $\mu_{\text{out}} \sim v^2$ . In order to match the parameter regime of the previously-presented astrophysical black holes, we shall assume that the thickness of the vortex's Higgs core,  $\sim m_h^{-1}$ , is smaller than the bubble radius,  $R \gg m_h^{-1}$ .

Let us now discuss the vacuum in the bubble interior,  $r < R$ , where  $\sigma = f$ . For  $\beta^2 > 0$ , this lowers the VEV of the Higgs as  $\rho_{\text{in}} = v_{\text{in}} = v \sqrt{1 - \frac{\beta^2 f^2}{\lambda^2 v^2}}$ . Of course, the inner vacuum still supports the vortex line but with a lower tension,  $\mu_{\text{in}} \sim v_{\text{in}}^2$ . Correspondingly, the difference between the string tensions in the bubble interior and the exterior is

$$\Delta\mu \equiv \mu_{\text{in}} - \mu_{\text{out}} \sim -\frac{\beta^2 f^2}{\lambda^2}. \quad (35)$$

We can mentally think of this shift in the tension as a scalar analog of the effect of the gravitational “red-shift”.

Thus, if a portion of the string of length  $\Delta L$  enters the bubble, the total potential energy of the system is lowered by  $\Delta E(L) = -\Delta L \Delta\mu$ . Therefore, there is an attractive force

$$F = \frac{\partial E}{\partial L} = -\Delta\mu, \quad (36)$$

which pulls the vortex line inside the bubble. Since inside the bubble the effective masses of the Higgs,  $m_h = \lambda v_{\text{in}}$ , and of the photon,  $m_\gamma = g v_{\text{in}}$ , are smaller than their vacuum counterparts, the portion of the vortex line absorbed by the bubble becomes thicker. This fattening is exhibited both by the Higgs and the magnetic cores. The ground state of the system of a bubble plus an infinite string is expected to be an axially-symmetric configuration with the vortex line piercing the bubble through the north and the south poles and with the inner portion being thicker than the outer one.

Notice that for  $\frac{\beta^2 f^2}{\lambda^2 v^2} > 1$ , the Higgs VEV in the interior,  $v_{\text{in}}$ , is practically zero (in reality, it is exponentially suppressed). In this case the bubble wall becomes a boundary between the Higgs and the Coulomb phases of  $U(1)_{\text{EM}}$  theory. If the vortex line crosses this boundary, the magnetic flux, which in the Higgs vacuum is confined in a tube, in the Coulomb phase becomes spread. The analytic and numeric studies of this phenomenon can be found in [55].

Applying to the present case, the vortex line piercing the vacuum bubble will spread within the bubble interior. However, the flux is conserved and continues to enter and exit the bubble in form of the vortex line. That is, passed the penetration point (say at the south pole), the flux spreads through the interior, reaching the maximum at the equatorial plane. Moving further up, the flux is gathering back and is exiting the bubble through the north pole in form of the string.

Notice that the energetics of the bubble-string interaction in the model (30) is determined by the Higgs core. Correspondingly, the trapping tendency persists even if the magnetic core of the vortex is much larger than the bubble radius.

All the above features can be smoothly extrapolated away from thin-wall and zero back-reaction approximations. With this extrapolation the outcome of the prototype system fully matches the estimates for black holes obtained earlier in the present paper.

First, as explained, in the thick-wall regime the bubble parameters match the one of a black hole with the identification  $f \rightarrow M_{\text{P}}$ . In particular, the relation between the size and mass is,

$$R \sim \frac{M}{f^2}. \quad (37)$$

Working in the regime  $v \ll f$  and  $\lambda \sim 1$ , we can see that the maximal value of the magnetic field sustained by the bubble is

$$B_{\text{max}} \sim \frac{f}{R}, \quad (38)$$

which with the substitution  $f \rightarrow M_{\text{P}}$  exactly matches the black hole case (17).

We shall now turn to numerical simulations of the above system.

## Numerics

In this subsection, we numerically illustrate the VTM mechanism using the simple prototype model (30). Visuals of the dynamics we are about to discuss can be found at the following URL to

which we refer the interested reader.

We begin by examining how a bubble moving through a “forest” of magnetic flux tubes can reach the maximum magnetic field it can sustain, eventually leaving a portion of the excessive flux behind. We also show how the magnetic field evolves during the merger of two such saturated bubbles when pierced by a flux tube. As we will see, most of the magnetic energy is dissipated in the process.

Concretely, we consider a bubble configuration in a global  $SU(N)$  theory, where the role of  $\Sigma$  is played by an adjoint representation, i.e. a Hermitian traceless  $N \times N$  matrix. Clearly, this choice does not affect the universal features of the VTM mechanism.

The potential  $V(\Sigma)$  in (30) shall be taken as [19–22, 50–52]:

$$V(\Sigma) = \frac{\alpha}{2} \text{Tr} \left[ f \Sigma - \Sigma^2 + \frac{I}{N} \text{Tr} \Sigma^2 \right]^2, \quad (39)$$

where  $I$  is the identity matrix,  $\alpha$  is a dimensionless coupling, and  $f$  denotes the characteristic scale.

The model admits multiple degenerate vacua satisfying the matrix equality ( $a, b$  are  $SU(N)$  indexes):

$$f \Sigma_a^b - (\Sigma^2)_a^b + \delta_a^b \frac{1}{N} \text{Tr} \Sigma^2 = 0, \quad (40)$$

which exhibit different symmetry-breaking patterns.

We investigate vacuum-bubble configurations interpolating from the  $SU(N)$ -symmetric vacuum outside of the bubble to an  $SU(N-1) \times U(1)$  vacuum inside the bubble. In the external region, the theory is in a gapped phase with mass squared  $m^2 = \alpha f^2$ . Inside the bubble, the spontaneous symmetry breaking gives rise to  $2(N-1)$  Goldstone species. The bubble domain wall separating the two phases has a thickness  $1/m$  and the tension  $m^3/(6\alpha)$ .

Such configurations can be constructed via the ansatz:

$$\Sigma = U^\dagger \Sigma_{\text{rad}} U, \quad (41)$$

where

$$\Sigma_{\text{rad}} = \frac{\sigma(x)}{\sqrt{N(N-1)}} \text{diag}[(N-1), -1, \dots, -1], \quad (42)$$

and

$$U = \exp \left[ i \chi(x) \hat{T} / \sqrt{2} \right]. \quad (43)$$

Here,  $\hat{T}$  denotes one of the generators broken by the ansatz (42), while  $\chi(x)$  represents the corresponding Goldstone mode. Notice that by reducing the  $\Sigma$ -field to  $\sigma(x)$  and  $\chi(x)$  components, the system effectively reduces to (31).

We focus on solutions of the form

$$\sigma(x) = f(r), \quad \chi(x) = \omega t, \quad (44)$$

describing a spherical bubble. The function  $f(r)$  satisfies  $f(0) \simeq f$  and  $f(\infty) = 0$ . The stability is ensured by the Goldstone charge  $Q$ . We solve for the bubble profile taking  $\alpha = 0.5$  and  $\omega = 0.5 m$ . Moreover, for practical purposes, in the following we specialize for the case  $N = 4$ .

*VTM Mechanism*

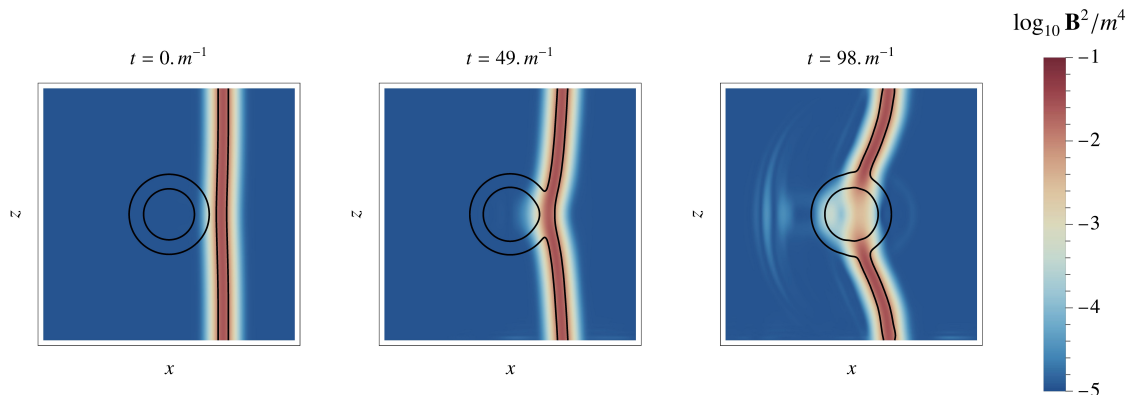


FIG. 1. 2D snapshots of the VTM dynamics. An infinite and straight flux tube aligned with the  $z$ -axis (its magnetic energy density in color) is captured by a nearby  $Q$ -ball type bubble. Black lines are isocontours of total energy density,  $|\epsilon| = 0.04 m^{-4}$ , which help to visualize the bubble.

We first demonstrate the essence of the VTM mechanism by considering a single, infinitely long flux tube near the bubble solution. Physically, capturing a single flux tube has negligible backreaction on the bubble. However, since a numerical implementation of a large separation of scales is challenging, we neglect the vortex's backreaction on the bubble by setting  $\beta = 0$  in (30) while evolving the adjoint field. We have confirmed that reintroducing the backreaction leaves the results qualitatively unchanged, simply adding a noise to the dynamics. Therefore, for clarity, we show the limit without backreaction.

Figure 1 depicts the evolution of the magnetic field energy density (in color), while the black contour marks  $|\epsilon| = 0.04 m^{-4}$ . As anticipated from the discussion following (35), the flux tube is attracted to the bubble. Inside the bubble, the VEV of the electromagnetic Higgs  $\rho$  is lower, reducing the effective gauge boson mass and allowing for a partial spreading of magnetic field lines. This is visible in the final panel, where the trapped portion of the flux tube has lower intensity. Notice that in the above numerical simulation and in what follows we fixed couplings such that the gauge- $U(1)_{EM}$  is still Higgsed in the interior of the bubble.

*Saturation of the Magnetic Field: A Walk Through the Forest*

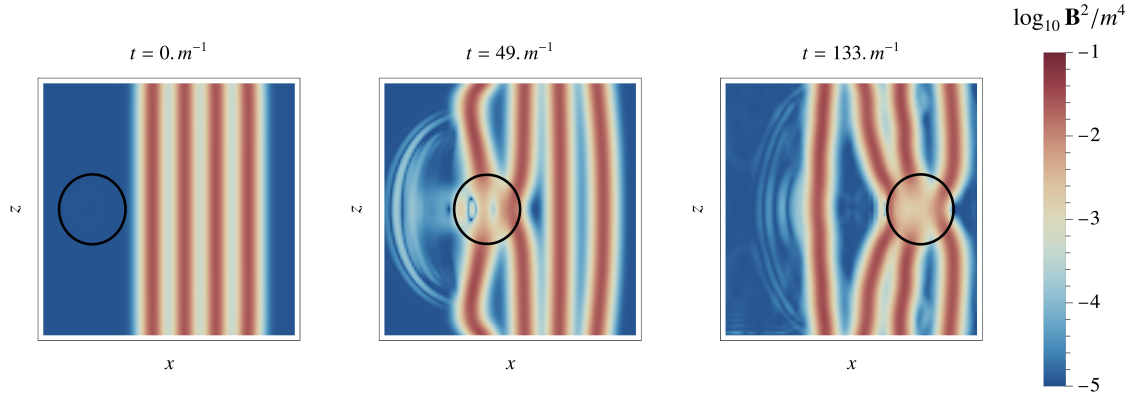


FIG. 2. 2D snapshots of a vortex-trapping bubble passing through a “forest” of flux tubes aligned with the  $x$ -axis. Their magnetic energy density is shown in red-blue. The black contour denotes the Q-ball bubble, identified by the iso-contour  $q = 10^{-1} m^3$ . After some time, the bubble saturates the magnetic field it can sustain, leaving behind one of the previously trapped flux tubes.

In our simulations, we set  $\lambda = 1$ ,  $v = 0.6 m$ ,  $\beta^2 = 0.4$ , and  $g = 1$ . While these values do not create a large hierarchy, they capture the core features of the VTM mechanism. Remarkably, for this choice, the bubble can only trap  $\mathcal{O}(1)$  flux tubes.

Figure 2 shows an example where we arrange a configuration of a series of infinite straight flux tubes with total winding number 4 along the  $z$ -axis and boost the bubble along  $x$  (first panel). The color map displays the magnetic energy density, and the black contour indicates the bubble’s location (corresponding to charge density  $q = 10^{-1} m^3$ ).

As before, the VTM mechanism traps flux tubes quite efficiently (second panel). Although a realistic black hole evolving in the galactic medium might involve more complex field configurations, our simplified setup is sufficient for illustrating the underlying physics of VTM phenomenon. Once the black-hole-analog bubble approaches its maximum possible field  $B_{\max}$ , it ceases to absorb additional flux. In our example, saturation is reached after capturing roughly three flux tubes (last panel in Fig. 2), causing the firstly-captured tube to be released. When nearing the saturation, the bubble can no longer confine more flux. Therefore, a part of the initially trapped flux - corresponding to the first captured vortex - is ejected and left behind.

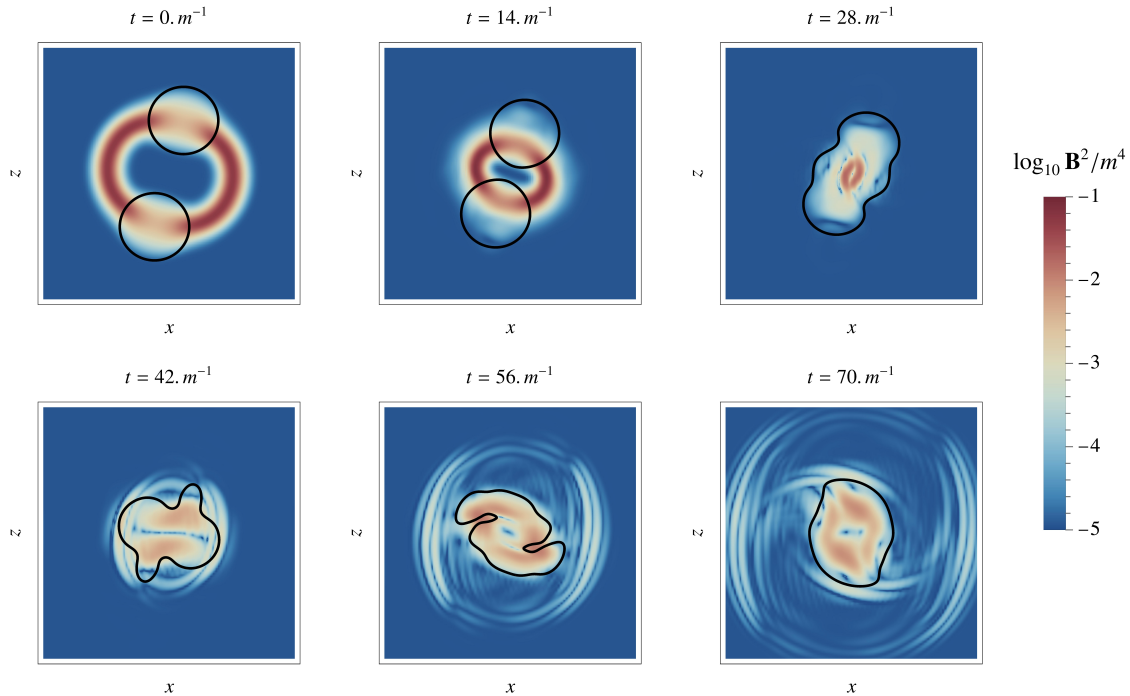


FIG. 3. Snapshots of two merging bubbles (black contours at  $q = 10^{-1} m^3$ ) in the presence of a circular flux-tube loop (red). As the bubbles merge, most of the magnetic field energy is radiated away.

### *Merger of Bubbles: Emission of Trapped Magnetic Field*

Finally, we turn to the merger dynamics in the adjoint sector, following a setup analogous to Ref. [22]. Two identical bubbles are placed at a separation of approximately one radius  $2R$ , with an impact parameter  $R$ , and boosted toward each other at  $v = 0.25c$ . Figure 3 shows black isocontours of the bubble location ( $q = 10^{-1} m^3$ ) and the flux-tube magnetic energy density in red. The evolution of the adjoint field is analogous to the one reported in Ref. [22] - to which we refer the interested reader for more details (see also URL1 and URL2 for visuals of the merger).

We initialize the magnetic vortex as a circular string loop piercing through both bubbles. After numerical relaxation, it is obviously no longer perfectly circular (first panel). When the bubbles merge, the loop can annihilate, releasing most of its energy in form of electromagnetic radiation (last three panels). Only a small fraction of the original magnetic field remains inside the merged bubble.

In the gravitational analog of this scenario (i.e. in mergers of highly-magnetized black holes), one might encounter flux tubes of more complicated shapes and topologies, potentially leading to way more complex dynamic than the one considered here. Nevertheless, this simplified setup shows that the bulk of the magnetic energy is radiated away during the merger, consistent with the expectation.

We have further verified that similar outcomes are provided by other geometries such as the case in which one of the bubbles is pierced by an infinitely long string perpendicular to its initial velocity. In this case, the merger dynamics leads to a highly-excited string which vibrates and emits radiation.

## VII. CONCLUSIONS AND OUTLOOK

In this paper we discussed some implications of non-zero photon mass within a consistent field-theoretic framework introduced in [1]. The photon mass is one of the most fundamental parameters of nature with an uncertain value. At first glance, it may appear that the photon mass is bounded from above by the inverse uniformity length of a magnetic field,  $l$ . According to this logic, the magnetic field of the galaxy, with the average strength  $B_g \sim 1 \mu\text{G}$  over the length scales  $l_g \gg 1 \text{ kpc}$ , would provide an upper bound  $m_\gamma < 3 \times 10^{-27} \text{ eV}$ . One would think that in the opposite case the contribution from the Proca energy would significantly affect the galactic plasma [25].

However, as argued in [1], the situation is profoundly different since the above bounds do not take into account the vortex structure of the magnetic field that is intrinsic to the theory with non-zero photon mass. Due to this structure, an uniform magnetic field of arbitrary extent,  $l \gg l_\gamma$ , can be sustained by a large number of overlapping Nielsen-Olesen magnetic vortexes. At the same time, the Proca energy is canceled by the winding of the Higgs phase.

This leaves us with milder bounds in the range  $m_\gamma \sim 10^{-14} - 10^{-17} \text{ eV}$ . That is, the uniformity of the galactic magnetic field over the length-scales  $l_g \gg 1 \text{ kpc}$ , is fully compatible with a much shorter Compton wavelength of the photon,  $l_\gamma \sim 10^{10} - 10^{13} \text{ cm}$  [1].

We notice that this range of the photon masses matches the sizes of supermassive astrophysical black holes. Correspondingly, it can generate a strong magnetic field via a new mechanism which we call VTm. The idea is that a black hole can substantially enhance its magnetic field by trapping the magnetic vortexes. The physical essence of trapping is similar to a trapping of a cosmic string by a black hole. The role of the cosmic string is played by the Higgs core of the magnetic vortex. The simple estimates show that the magnetic field achieved in this way can saturate the upper bound (1) on the magnetic capacity of a black hole.

The actual formation mechanism of such black holes is a separate question depending on the details of the cosmological scenario. However, there exists a minimal model-independent contribution from the exposure of a black hole to the wind of the vortex network composing the magnetic field of the galaxy.

Indeed, according to the massive photon scenario of [1], the galactic magnetic field represents a densely populated forest of vortexes with overlapping magnetic cores. Notice that this is not an additional assumption but a dynamically-generated structure of the galactic magnetic field imposed by a non-zero photon mass.

These vortexes are expected to be trapped and collected by a black hole. We estimate that

the magnetic field accumulated in this way over a cosmic time is (28). Notice that this minimal contribution to the magnetic field of a black hole is purely the effect coming from the galactic magnetic field, independent of the existence of any electromagnetic plasma in the Universe. The presence of plasma is expected to provide further enhancement effects which require separate studies.

The VTM effect is of direct relevance for magnetic field induced particle acceleration scenarios such as the ones based on Fermi [3–6] or the Blandford-Znajek [7, 8] mechanisms. Another promising mechanism of direct relevance is provided by the magneto-centrifugal acceleration.

The near-saturated value of the magnetic field provided by the VTM can have significant effects in black hole mergers. The mergers of strongly magnetized black holes are expected to be accompanied by a highly intense electromagnetic radiation of wavelength  $\sim R$  with the power that can potentially reach nearly-Planckian values (29). This radiation is expected to carry away an order-one fraction of the magnetic energy which for the saturated value (1) is comparable to the black hole mass.

We have provided an explicit numerical simulation of VTM effect within a simple toy model (visuals can be found at the following URL). In this model the role of a black hole is played by a saturon bubble introduced as a black hole prototype in the earlier works [19–22]. While this soliton shares the relevant key properties with a black hole, it is easier to analyse. In this model, we gave a full analytic realization of the VTM phenomenon and also performed the numerical simulation of its real-time dynamics. With the proper mapping of the parameters, the system reproduces the expected features of VTM in black holes. As a side remark, apart of being an useful theoretical test prototype for a black hole, a highly-magnetized vacuum bubble would be a rather interesting astrophysical object. In particular, it can mimic features of highly-magnetized black holes. It therefore would be proper to identify such solitons in motivated extensions of the Standard Model.

The magnetodynamics of mergers of VTM black holes shares some features observed in the simulations in analog systems of highly-spinning saturon bubbles [24], motivated by the alternative magnetization scenario of [21, 22].

Finally we would like to remark about some further obvious implications of the considered scenario to be looked at. The first is the so-called superradiance [56–60] which manifests in amplification of radiation by a rotating black hole of bosonic particles with Compton wavelengths comparable to the black hole radius. This phenomenon has been discussed for hypothetical particles such as the axion-like pseudo-scalars [61] or hidden sector “dark photons” [62]. However, to our knowledge, this effect has never been applied to photons, since ordinarily they are considered to be massless. In contrast, the scenario considered here is ready-made for this effect, since the photon mass can be in the right ballpark for supermassive black holes. We thus expect that in resonant cases, photon superradiance can open up an additional energy loss channel for a spinning black hole. This may impose restrictions on the parameters of the theory.

Another natural consequence of VTM would be the emission of gravitational waves from the vortexes that spin with a black hole and, in particular, from their Higgs cores. Cosmic string loops are well known potential sources of gravitational waves (see, e.g, [63–65]). The gravitational

radiation from strings trapped in spinning black holes has also been considered [47, 48]. This can have direct implications for the VTM scenario. All the above effects require quantifications by precision studies.

**Acknowledgments** We acknowledge the useful discussions and ongoing collaborations [23, 24, 30] with Juan Sebastian Valbuena-Bermudez, Florian Kühnel and Maximilian Bachmaier. We are grateful to Elisa Resconi for discussions about IceCube and related topics. We thank Roger Blandford for illuminating communication about the magnetic fields in black holes at early stage of this work.

Z.O. would like to thank Arnold Sommerfeld Center, Ludwig Maximilians University and Max Planck Institute for Physics for hospitality during the work on this project.

The work of G.D. was supported in part by the Humboldt Foundation under Humboldt Professorship Award, by the European Research Council Gravities Horizon Grant AO number: 850 173-6, by the Deutsche Forschungsgemeinschaft (DFG, German Research Foundation) under Germany’s Excellence Strategy - EXC-2111 - 390814868, and Germany’s Excellence Strategy under Excellence Cluster Origins. The work of Z.O. was supported by Shota Rustaveli National Science Foundation of Georgia (SRNSFG). Grant: FR-23-18821 and DAAD scholarship within the program Research Stays for University Academics and Scientists, 2024 (ID: 57693448).

Disclaimer: Funded by the European Union. Views and opinions expressed are however those of the authors only and do not necessarily reflect those of the European Union or European Research Council. Neither the European Union nor the granting authority can be held responsible for them.

- 
- [1] Eric Adelberger, Gia Dvali, and Andrei Gruzinov, “Photon mass bound destroyed by vortices,” *Phys. Rev. Lett.* **98**, 010402 (2007), arXiv:hep-ph/0306245.
  - [2] Holger Bech Nielsen and P. Olesen, “Vortex Line Models for Dual Strings,” *Nucl. Phys. B* **61**, 45–61 (1973).
  - [3] Enrico Fermi, “On the Origin of the Cosmic Radiation,” *Phys. Rev.* **75**, 1169–1174 (1949).
  - [4] A. R. Bell, “The Acceleration of cosmic rays in shock fronts. I,” *Mon. Not. Roy. Astron. Soc.* **182**, 147–156 (1978).
  - [5] A. R. Bell, “The acceleration of cosmic rays in shock fronts. II,” *Mon. Not. Roy. Astron. Soc.* **182**, 443–455 (1978).
  - [6] R. W. Lessard *et al.*, “Constraints on cosmic ray origin theories from TeV gamma-ray observations,” in *25th International Cosmic Ray Conference* (1997) arXiv:astro-ph/9706131.
  - [7] R. D. Blandford and R. L. Znajek, “Electromagnetic extractions of energy from Kerr black holes,” *Mon. Not. Roy. Astron. Soc.* **179**, 433–456 (1977).
  - [8] Alexander Tchekhovskoy, Jonathan C. McKinney, and Ramesh Narayan, “General Relativistic Modeling of Magnetized Jets from Accreting Black Holes,” *J. Phys. Conf. Ser.* **372**, 012040 (2012), arXiv:1202.2864 [astro-ph.HE].

- [9] Zaza Osmanov, Andria D. Rogava, and Gianluigi Bodo, “On efficiency of particle acceleration by rotating magnetospheres in AGN,” *Astron. Astrophys.* **470**, 395 (2007), arXiv:astro-ph/0609327.
- [10] Zaza Osmanov, “Is very high energy emission from the BL Lac 1ES 0806+524 centrifugally driven?” *New Astron.* **15**, 351–355 (2010), arXiv:0901.1235 [astro-ph.HE].
- [11] F. M. Rieger and K. Mannheim, “Particle acceleration by rotating magnetospheres in active galactic nuclei,” *Astron. Astrophys.* **353**, 473 (2000), arXiv:astro-ph/9911082.
- [12] Jihyun Kim, Dongsu Ryu, Soonyoung Roh, Jihoon Ha, and Hyesung Kang, “Propagation of ultra-high-energy cosmic rays in the magnetized cosmic web,” *PoS ICRC2019*, 315 (2020), arXiv:1909.02189 [astro-ph.HE].
- [13] Kohta Murase, Markus Ahlers, and Brian C. Lacki, “Testing the Hadronuclear Origin of PeV Neutrinos Observed with IceCube,” *Phys. Rev. D* **88**, 121301 (2013), arXiv:1306.3417 [astro-ph.HE].
- [14] M. G. Aartsen *et al.* (IceCube), “First observation of PeV-energy neutrinos with IceCube,” *Phys. Rev. Lett.* **111**, 021103 (2013), arXiv:1304.5356 [astro-ph.HE].
- [15] M. G. Aartsen *et al.* (IceCube), “Evidence for High-Energy Extraterrestrial Neutrinos at the IceCube Detector,” *Science* **342**, 1242856 (2013), arXiv:1311.5238 [astro-ph.HE].
- [16] R. Abbasi *et al.* (IceCube), “Observation of high-energy neutrinos from the Galactic plane,” *Science* **380**, adc9818 (2023), arXiv:2307.04427 [astro-ph.HE].
- [17] S. Aiello *et al.* (KM3NeT), “Observation of an ultra-high-energy cosmic neutrino with KM3NeT,” *Nature* **638**, 376–382 (2025).
- [18] P. Padovani *et al.*, “High-energy neutrinos from the vicinity of the supermassive black hole in NGC 1068,” *Nature Astron.* **8**, 1077–1087 (2024), arXiv:2405.20146 [astro-ph.HE].
- [19] Gia Dvali, “Entropy Bound and Unitarity of Scattering Amplitudes,” *JHEP* **03**, 126 (2021), arXiv:2003.05546 [hep-th].
- [20] Gia Dvali, Oleg Kaikov, and Juan Sebastián Valbuena Bermúdez, “How special are black holes? Correspondence with objects saturating unitarity bounds in generic theories,” *Phys. Rev. D* **105**, 056013 (2022), arXiv:2112.00551 [hep-th].
- [21] Gia Dvali, Florian Kühnel, and Michael Zantedeschi, “Vortices in Black Holes,” *Phys. Rev. Lett.* **129**, 061302 (2022), arXiv:2112.08354 [hep-th].
- [22] Gia Dvali, Oleg Kaikov, Florian Kühnel, Juan Sebastian Valbuena-Bermudez, and Michael Zantedeschi, “Vortex Effects in Merging Black Holes and Saturons,” *Phys. Rev. Lett.* **132**, 151402 (2024), arXiv:2310.02288 [hep-ph].
- [23] F. Kuhnel and J. S. Valbuena-Bermudez, Private Communication.
- [24] Gia Dvali, Juan Sebastian Valbuena-Bermudez, and Michael Zantedeschi, “Simulations of mergers of spinning magnetized saturons,” In progress.
- [25] Yoshio Yamaguchi, “A composite theory of elementary particles,” *Progress of Theoretical Physics Supplement* **11**, 1–36 (1959), <https://academic.oup.com/ptps/article-pdf/doi/10.1143/PTPS.11.1/5445105/11-1.pdf>.
- [26] G. V. Chibisov, “Astrophysical upper limits on the photon rest mass,” *Sov. Phys. Usp.* **19**, 624–626 (1976).
- [27] R. Lakes, “Experimental limits on the photon mass and cosmic magnetic vector potential,” *Phys. Rev. Lett.* **80**, 1826–1829 (1998).
- [28] Jun Luo, Liang-Cheng Tu, Zhong-Kun Hu, and En-Jie Luan, “New experimental limit on the photon rest mass with a rotating torsion balance,” *Phys. Rev. Lett.* **90**, 081801 (2003).
- [29] Gia Dvali, “Three-form gauging of axion symmetries and gravity,” (2005), arXiv:hep-th/0507215.

- [30] Maximilian Bachmaier and Juan Sebastian Valbuena Bermudez, Private communications, work in progress.
- [31] E. R. Williams, J. E. Faller, and H. A. Hill, “New experimental test of coulomb’s law: A laboratory upper limit on the photon rest mass,” *Phys. Rev. Lett.* **26**, 721–724 (1971).
- [32] A. Vilenkin, “Gravitational Field of Vacuum Domain Walls and Strings,” *Phys. Rev. D* **23**, 852–857 (1981).
- [33] Mukunda Aryal, L. H. Ford, and Alexander Vilenkin, “Cosmic Strings and Black Holes,” *Phys. Rev. D* **34**, 2263 (1986).
- [34] Ana Achucarro, Ruth Gregory, and Konrad Kuijken, “Abelian Higgs hair for black holes,” *Phys. Rev. D* **52**, 5729–5742 (1995), arXiv:gr-qc/9505039.
- [35] S. Lonsdale and I. Moss, “The Motion of Cosmic Strings Under Gravity,” *Nucl. Phys. B* **298**, 693–700 (1988).
- [36] Jean-Pierre De Villiers and Valeri P. Frolov, “Gravitational capture of cosmic strings by a black hole,” *Int. J. Mod. Phys. D* **7**, 957–967 (1998), arXiv:gr-qc/9711045.
- [37] Jean-Pierre De Villiers and Valeri P. Frolov, “Gravitational scattering of cosmic strings by nonrotating black holes,” *Class. Quant. Grav.* **16**, 2403–2425 (1999), arXiv:gr-qc/9812016.
- [38] Martin Snajdr and Valeri P. Frolov, “Capture and critical scattering of a long cosmic string by a rotating black hole,” *Class. Quant. Grav.* **20**, 1303–1320 (2003), arXiv:gr-qc/0211018.
- [39] Florian Dubath, Mairi Sakellariadou, and Claude Michel Viallet, “Scattering of cosmic strings by black holes: Loop formation,” *Int. J. Mod. Phys. D* **16**, 1311–1325 (2007), arXiv:gr-qc/0609089.
- [40] Valeri P. Frolov, S. Hendy, and A. L. Larsen, “How to create a 2-D black hole,” *Phys. Rev. D* **54**, 5093–5102 (1996), arXiv:hep-th/9510231.
- [41] Takahisa Igata, Hideki Ishihara, Masataka Tsuchiya, and Chul-Moon Yoo, “Rigidly rotating string sticking in a kerr black hole,” *Phys. Rev. D* **98**, 064021 (2018).
- [42] Gia Dvali and Oriol Pujolas, “Micro Black Holes and the Democratic Transition,” *Phys. Rev. D* **79**, 064032 (2009), arXiv:0812.3442 [hep-th].
- [43] Gia Dvali, “Nature of Microscopic Black Holes and Gravity in Theories with Particle Species,” *Int. J. Mod. Phys. A* **25**, 602–615 (2010), arXiv:0806.3801 [hep-th].
- [44] Gia Dvali, “Black Holes and Large N Species Solution to the Hierarchy Problem,” *Fortsch. Phys.* **58**, 528–536 (2010), arXiv:0706.2050 [hep-th].
- [45] Gia Dvali and Michele Redi, “Black Hole Bound on the Number of Species and Quantum Gravity at LHC,” *Phys. Rev. D* **77**, 045027 (2008), arXiv:0710.4344 [hep-th].
- [46] David F. Chernoff and S. H. Henry Tye, “Cosmic String Detection via Microlensing of Stars,” (2007), arXiv:0709.1139 [astro-ph].
- [47] Hengrui Xing, Yuri Levin, Andrei Gruzinov, and Alexander Vilenkin, “Spinning black holes as cosmic string factories,” *Phys. Rev. D* **103**, 083019 (2021), arXiv:2011.00654 [astro-ph.HE].
- [48] Heling Deng, Andrei Gruzinov, Yuri Levin, and Alexander Vilenkin, “Simulating cosmic string loop captured by a rotating black hole,” *Phys. Rev. D* **107**, 123016 (2023), arXiv:2303.02726 [gr-qc].
- [49] Gia Dvali and Cesar Gomez, “Black Hole’s Quantum N-Portrait,” *Fortsch. Phys.* **61**, 742–767 (2013), arXiv:1112.3359 [hep-th].
- [50] Gia Dvali, “Area Law Saturation of Entropy Bound from Perturbative Unitarity in Renormalizable Theories,” *Fortsch. Phys.* **69**, 2000090 (2021), arXiv:1906.03530 [hep-th].
- [51] Gia Dvali, “Unitarity Entropy Bound: Solitons and Instantons,” *Fortsch. Phys.* **69**, 2000091 (2021), arXiv:1907.07332 [hep-th].

- [52] Gia Dvali and Otari Sakhelashvili, “Black-hole-like saturons in Gross-Neveu,” *Phys. Rev. D* **105**, 065014 (2022), arXiv:2111.03620 [hep-th].
- [53] T. D. Lee and Y. Pang, “Nontopological solitons,” *Phys. Rept.* **221**, 251–350 (1992).
- [54] Sidney R. Coleman, “Q-balls,” *Nucl. Phys. B* **262**, 263 (1985), [Addendum: *Nucl.Phys.B* 269, 744 (1986)].
- [55] Gia Dvali and Juan Sebastián Valbuena-Bermúdez, “Erasure of strings and vortices,” *Phys. Rev. D* **107**, 035001 (2023), arXiv:2212.07535 [hep-th].
- [56] Ya. B. Zeldovich and Alexei A. Starobinsky, “Particle production and vacuum polarization in an anisotropic gravitational field,” *Zh. Eksp. Teor. Fiz.* **61**, 2161–2175 (1971).
- [57] Charles W. Misner, “Interpretation of gravitational-wave observations,” *Phys. Rev. Lett.* **28**, 994–997 (1972).
- [58] A. A. Starobinsky, “Amplification of waves reflected from a rotating “black hole”.” *Sov. Phys. JETP* **37**, 28–32 (1973).
- [59] Steven L. Detweiler, “KLEIN-GORDON EQUATION AND ROTATING BLACK HOLES,” *Phys. Rev. D* **22**, 2323–2326 (1980).
- [60] Jacob D. Bekenstein and Marcelo Schiffer, “The Many faces of superradiance,” *Phys. Rev. D* **58**, 064014 (1998), arXiv:gr-qc/9803033.
- [61] Asimina Arvanitaki, Savvas Dimopoulos, Sergei Dubovsky, Nemanja Kaloper, and John March-Russell, “String Axiverse,” *Phys. Rev. D* **81**, 123530 (2010), arXiv:0905.4720 [hep-th].
- [62] Nils Siemonsen, Cristina Mondino, Daniel Egana-Ugrinovic, Junwu Huang, Masha Baryakhtar, and William E. East, “Dark photon superradiance: Electrodynamics and multimessenger signals,” *Phys. Rev. D* **107**, 075025 (2023), arXiv:2212.09772 [astro-ph.HE].
- [63] A. Vilenkin, “Gravitational radiation from cosmic strings,” *Phys. Lett. B* **107**, 47–50 (1981).
- [64] Tanmay Vachaspati and Alexander Vilenkin, “Gravitational Radiation from Cosmic Strings,” *Phys. Rev. D* **31**, 3052 (1985).
- [65] Jose J. Blanco-Pillado and Ken D. Olum, “Stochastic gravitational wave background from smoothed cosmic string loops,” *Phys. Rev. D* **96**, 104046 (2017), arXiv:1709.02693 [astro-ph.CO].